Brazilian Journal of Physics (2026) 56:102
https://doi.org/10.1007/s13538-026-02009-7

Cosmic Strings and Negative Λ: Probing the Infant Universe in Einstein-Æther Theory

A. Oliveira Castro Júnior[1] · G. A. Monerat[1] · F. G. Alvarenga[2] · G. Oliveira-Neto[3] · F. R. Manhães[1] · E. V. Corrêa Silva[4] · V. J. Monteiro[1] · J. C. G. Tedesco[5]

Received: 23 September 2025 / Accepted: 5 January 2026

Abstract

In this work, we analyze a quantized cosmological model within the framework of Einstein-Aether theory, with matter content described by a cosmic string fluid and the presence of a negative cosmological constant. The quantization is performed using the minisuperspace formalism with a perfect fluid via the velocity potentials approach, which allows for the interpretation of the fluid-associated variable as an internal time. The resulting Wheeler-DeWitt equation is solved, yielding normalizable eigenstates and associated wave packets. Employing both the many-worlds and the de Broglie-Bohm interpretations, we determine the dynamics of the scale factor and the behavior of the quantum potential. The results demonstrate the absence of singularities in our model, and the independence of the probability density with respect to the spatial curvature.

Keywords Cosmic strings · Quantum cosmology · Wheeler-DeWitt equation

1 Introduction

Quantum cosmology aims to describe the Universe as a whole through quantum theory, particularly when addressing issues like the initial singularity or the initial conditions for spacetime [1–3].

The Hamiltonian formulation of General Relativity, developed in the 1960s by Arnowitt, Deser, and Misner (ADM formalism) [4], describes the dynamics of the system via the time evolution of a 3D hypersurface (where fields are defined) and the Wheeler-DeWitt equation governing the wave function of the Universe [5]. In minisuperspace models, infinite degrees of freedom are fixed, leaving the

✉ G. A. Monerat
monerat@uerj.br

A. Oliveira Castro Júnior
alessandroocj@protonmail.com

F. G. Alvarenga
flavio.alvarenga@ufes.br

G. Oliveira-Neto
gilneto@fisica.ufjf.br

F. R. Manhães
fabio.ramos@iprj.uerj.br

E. V. Corrêa Silva
profeduvasquezuerj@gmail.com.br

V. J. Monteiro
vagner.jandre@iprj.uerj.br

J. C. G. Tedesco
tedesco@iprj.uerj.br

1 Departamento de Modelagem Computacional, Instituto Politécnico, Universidade do Estado do Rio de Janeiro, 28625-570 Nova Friburgo, RJ, Brazil

2 Departamento de Física, Centro de Ciências Exatas, Universidade Federal do Espírito Santo, 29075-910 Vitória, ES, Brazil

3 Departamento de Física, Instituto de Ciências Exatas, Universidade Federal de Juiz de Fora, 36036-330 Juiz de Fora, Minas Gerais, Brazil

4 Departamento de Matemática, Física e Computação, Faculdade de Tecnologia, Universidade do Estado do Rio de Janeiro, 27537-000 Resende, RJ, Brazil

5 Departamento de Engenharia Mecânica e Energia, Instituto Politécnico, Universidade do Estado do Rio de Janeiro, 28625-570 Nova Friburgo, RJ, Brazil

Published online: 24 February 2026

scale factor and matter content as key variables. Alvarenga et al. [6] showed that, for a perfect fluid with barotropic equation of state ($p = \alpha\rho$), it is possible to obtain analytical solutions for the Wheeler-DeWitt equation for Friedmann-Lemaître-Robertson-Walker (FLRW) models [6]. In these specific models, for any value of $\alpha < 1$, nonsingular quantum Universes (with *bounces*) may arise, and, particularly, the Universe shows an accelerated expansion if $-1 < \alpha < -1/3$. These results underscore the role of the Wheeler-DeWitt equation in probing quantum emerging universes and exotic matter.

The likelihood of Lorentz symmetry violation at certain energy scales [7] has spurred interest in gravitational theories that incorporate this breaking, such as the Einstein-Æther theory [8, 9]. This theory modifies General Relativity by introducing a unitary timelike vector field u^a that defines a preferred local reference frame in each point of spacetime. Lorentz symmetry breaking also implies a possible rethinking of several subjects such as dark matter and dark energy, cosmic microwave background, and cosmic inflation [10–12]. On the other hand, describing the Universe in Einstein-Æther theory may lead to models with new singularities [13]. Notwithstanding, recent works motivate the investigation regarding the Einstein-Æther theory. Researchers using data from the Event Horizon Telescope(EHT) were able to find a black hole solution using Einstein-Æther gravity that agrees with the shadow size of the EHT M87* [14] given that the parameters of the theory are defined within a certain range. In a recent investigation, Bokhari et al. [15] used observational data to explore the vacuum electrodynamics and the plasma magnetosphere of a magnetized neutron star using Einstein-Æther gravity to find observational constraints for the upper limits of the Einstein-Æther theory parameters. Bairagi [16] builds a cosmological model in Einstein-Æther gravity using a non-canonical scalar field type dark energy, and its efficiency is tested by comparing its predictions to observational data from three compilations of the Type Ia supernovae dataset, namely, Union2.1, JLA and Pantheon. The study leads to the conclusion that the model fits the observational data properly and is able to reproduce the accelerated expansion of the Universe. Adam et al. [17] numerically built time stationary and rotating black hole solutions in Einstein-Æther theory and study their properties, focusing on two phenomenologically viable regions in the parameter space in which some couplings of the theory are large, which could suggest significant deviations from General Relativity. However, the main argument and result of the work is that even in these regimes, rotating black holes approach the GR Kerr metric remarkably well. This happens because the aether field dynamically organizes itself to be either nearly "torsion-free" or "torsion-and-expand"-free.

On the other hand, it is also crucial to emphasize our preference towards a negative cosmological constant ($\Lambda < 0$) [18–22]. From a quantum point of view, a negative constant induces an effective potential that allows the existence of bound states in the Wheeler-DeWitt equation, enabling normalizable solutions and a coherent description of the primordial universe without singularities. Some recent works may support the study of models with a negative cosmological constant. In 2024, Akarsu et al. [23] tested a new cosmological model known as Λ_SCDM, which considers the possibility that the Universe has undergone a transition from a negative (AdS) to a positive (dS) vacuum energy at redshift $z \approx 1.7$, that is, a sign-switching of the cosmological constant. The paper shows that this assumption has significantly improved the fit to observational data. Based on James Webb Space Telescope [24] observations, the authors investigate a dynamical dark energy model featuring a quintessence field with a negative cosmological constant, also described as an Anti-de Sitter (AdS) vacuum, as its ground state. They find that such models naturally affect the galaxy UV luminosities in the redshift range $10 \leq z \leq 15$ needed to match the JWST observations. The authors of [25] studied a cosmological model featuring a negative cosmological constant (AdS vacuum) in conjunction with a dynamical quintessence dark energy field, exploring how future radio astronomy can constrain such a scenario. Their work shows that existing galaxy survey data already permit negative cosmological constant models, particularly those with a phantom-like dark energy component that favors a higher value for the Hubble constant, H_0. In [26] and [27] the authors considered models featuring a negative cosmological constant that leads to potential explanations of some of the JWST observational data.

In order to introduce matter content into a canonical model, one may use Schutz's perfect fluid formalism [28–30], in which velocity potentials are assigned to the fluid. Its conjugate momentum enters the action linearly thus allowing the fluid to act as an internal clock, converting the Wheeler-DeWitt equation into a Schrödinger-like form for easier quantum analysis of the scale factor's dynamics.

Cosmic strings are a particular instance of an exotic fluid to be studied. They are one-dimensional topological defects foreseen in Great Unified Theories, appearing when symmetries are broken in phase transitions of the early Universe. The fluid related to cosmic strings is described by the equation of state $p = w\rho$, with $w = -1/3$. (Other fluids such as stiff matter and radiation are characterized by $w = 1$ and $w = 1/3$, respectively.) Kibble [31] was the first to describe these strucurein the 1970's. In the 80's, cosmic strings were considered as the seeds for large scale structures: since they are linear objects, they could have been the cause the formation of galaxies and clusters. Their presence could be traced through detectable fingerprints, for example, in anisotropic anomalies in the cosmic microwave background radiation. Nonetheless, it was found through observations such as COBE and WMAP that cosmic strings do not contribute significantly to the current anisotropies [32–35]. Yet, modern theories (including the idea of *superstrings*) suggest that string nets would have evolved in the early Universe and could represent 10% of the primordial anisotropies. Despite not fully explaining structures formation, cosmic strings are still a valuable component of primordial cosmology models [20, 36].

In this work, we analyze a quantized cosmological model within the framework of Einstein-Aether theory, with matter content described by a cosmic string fluid and negative cosmological constant [37–41]. Its quantization is performed using the minisuperspace formalism with a perfect fluid via the velocity potentials approach, which allows for the interpretation of the fluid-associated variable as an internal time. The resulting Wheeler-DeWitt equation is solved, yielding normalizable eigenstates and associated wave packets. Employing both the many-worlds and the de Broglie-Bohm interpretations, we determine the dynamics of the scale factor and the behavior of the quantum potential. The results demonstrate the absence of singularities in our model, and the independence of the probability density on the spatial curvature.

This article is organized as follows. In Section 2, we present our classical Einstein-Æther cosmological model with negative cosmological constant and cosmic strings fluid, derived from its complete Hamiltonian. In Section 3 we perform the canonical quantization of the model and obtain solutions to the Wheeler-DeWitt equation; the eigenvalues and eigenfunction are obtained analytically, and normalizable wave packets are built. In Section 4, we derive the expectation value of the scale factor of the Universe and its uncertainty, in the many-worlds interpretation of quantum mechanics, and the quantum trajectories related to the Universe's scale factor within the framework of the de Broglie-Bohm interpretation. Section 5 is devoted to our concluding remarks.

2 The Classical Model

Our starting point is the Einstein-Aether action [13]:

$$S_{\text{A-E}} = \frac{1}{16\pi G}\Bigg[\int_{\mathcal{M}} d^4x\sqrt{-g}\,(R-2\Lambda) + 2\int_{\partial\mathcal{M}} d^3x\sqrt{h}\,h^{ab}B_{ab} - K^{ab}{}_{mn}\nabla_a u^m \nabla_b u^n + \lambda(u^a u_a + 1)\Bigg]. \tag{1}$$

This is a generalization of the Einstein-Hilbert action that explicitly incorporates a unit timelike dynamical vector field u^a, called the ether field. This field spontaneously breaks the local Lorentz symmetry, by defining a preferred direction in spacetime at each point while maintaining, however, the general covariance of the theory. R is the scalar curvature derived from the spacetime metric $g_{\mu\nu}$, h_{ab} is the induced 3-metric on the boundary $\partial\mathcal{M}$, and B_{ab} is the extrinsic curvature; furthermore, G is the gravitational constant, g is the determinant of $g_{\mu\nu}$, and h is the determinant of h_{ab}. The tensor K^{ab}_{mn} encompasses the coupling constants of the model,

$$K^{ab}{}_{mn} = c_1\, g^{ab} g_{mn} + c_2\, \delta^a_m \delta^b_n + c_3\, \delta^a_n \delta^b_m + c_4\, u^a u^b g_{mn}. \tag{2}$$

The coefficients c_i are dimensionless constants that couple the ether field to the metric, and λ is a Lagrange multiplier that imposes the normalization condition $u^a u_a = -1$ upon the ether field. The matter content can be phenomenologically included by Schutz's action [28–30]

$$S_M = \int_{\mathcal{M}} d^4x\,\sqrt{-g}\,p\,, \tag{3}$$

which makes possible to describe in terms of scalar potentials the pressure p of a cosmic strings relativistic fluid ($p = -\rho/3$).

The classical model is built considering an isotropic and homogeneous Universe, characterized by a FLRW metric

$$ds^2 = -N^2(t)\,dt^2 + a^2(t)\left[\frac{dr^2}{1-kr^2} + r^2(d\theta^2 + \sin^2\theta\, d\phi^2)\right]. \tag{4}$$

in which $a(t)$ is the scale factor and $N(t)$ is the lapse function. The complete action of the model can be reduced by canonical methods [42]:

$$\mathcal{S} = \int dt\,\left[\dot{a}\,p_a + \dot{T}\,p_T - NH\right]\,, \tag{5}$$

where

$$H = -\frac{\sigma\,p_a^2}{12a(\beta+2)} - \frac{6ka}{\sigma} + \Lambda a^3 + a\,p_T \tag{6}$$

is the so-called super-Hamiltonian, in which p_a and p_T are the momenta canonically conjugated to the scale factor a and to the remaining degree of freedom T of the cosmic string fluid, respectively. The lapse function N plays the role of a Lagrange multiplier, which determines the super-Hamiltonian constraint:

$$H = 0\,. \tag{7}$$

On the other hand, the parameters β and σ are remnants of the Einstein-Aether theory, defined from the coupling constants and rescaling of the effective (Newtonian) gravitational constant G_N:

$$\beta = c_1 + 3c_2 + c_3 \quad \text{e} \quad \sigma = 1 - \frac{c_1 + c_4}{2}\,; \tag{8}$$

$$G_N = \frac{G}{\sigma}\,. \tag{9}$$

For details on the derivation of the super-Hamiltonian (6), see [6, 43–45]. In this work, we assume $16\pi G_N = 1$. Even thought the condition $\sigma < 0$ is mathematically possible, it is physically ruled out by the constraints imposed on the Einstein-Aether theory [43]. One example of such constraint is that the effective gravitational constant $G_N = G/\sigma$ would become negative, which is physically unacceptable. Hence we will consider $0 < \sigma < 1$.

It is convenient to introduce a new parametrization of the lapse function by writing it as $N\,a^{-1}$. Thus, the action retains the form (5), but the super-Hamiltonian is modified to

$$H = -\frac{\sigma\, p_a^2}{12a^2(\beta + 2)} - \frac{6k}{\sigma} + \Lambda a^2 + p_T\,, \tag{10}$$

which can be written in terms of new parameters *m* and w_k, defined as

$$m = \frac{6(\beta + 2)}{\sigma}, \quad \text{and} \quad w_k = \sqrt{\frac{2k}{\beta + 2}}\,. \tag{11}$$

This leads to

$$H = -\frac{p_a^2}{2ma^2} - \frac{mw_k^2}{2} + \Lambda a^2 + p_T\,. \tag{12}$$

It is crucial to use the following canonical transformation to avoid ordering problems,

$$a = \sqrt{2x}, \;\; \text{and} \;\; p_a = p_x\, a\,, \tag{13}$$

the generating function of which is

$$F = \frac{1}{2} p_x a^2\,. \tag{14}$$

From this point on, we will refer to *x* as the “scale factor”. Applying the canonical transformation (13) to (12) one obtains

$$H = -\frac{p_x^2}{2m} - \frac{mw_k^2}{2} + 2\Lambda x + p_T. \tag{15}$$

The classical equations of motion are

$$\begin{cases} \dot{x} = & \dfrac{\partial(NH)}{\partial p_x} = -\dfrac{p_x}{m}\,; \\ \dot{p}_x = & -\dfrac{\partial(NH)}{\partial x} = -2\Lambda; \\ \dot{T} = & \dfrac{\partial(NH)}{\partial p_T} = 1\,; \\ \dot{p}_T = & -\dfrac{\partial(NH)}{\partial T} = 0, \end{cases} \tag{16}$$

together with the super-Hamiltonian constraint

$$H = -\frac{p_x^2}{2m} - \frac{mw_k^2}{2} + 2\Lambda x + p_T = 0\,. \tag{17}$$

The system described by (16) is integrable and has as solution

$$x(t) = x_0 - \frac{p_{x_0}}{m} t + \frac{\Lambda}{m} t^2\,. \tag{18}$$

The gauge choice $t = T$ implies that $N = 1$, and that p_T is a constant of motion.

For our model with $\Lambda < 0$ and $m > 0$, the classical solution (18) is singular; i.e. for a finite time *t* we have $x(t) = 0$. Particularly, it is quite intriguing that for this model the classical dynamics of the evolution of the scale factor of the Universe is independent of the sign of the spatial curvature *k*.

3 The Quantum Model

The quantization of the model in the Wheeler–DeWitt scheme [46, 47] consists in replacing

$$\hat{p}_x \to -i\hbar\frac{\partial}{\partial x} \;\text{and}\; \hat{p}_T \to -i\hbar\frac{\partial}{\partial T}\;, \tag{19}$$

in the super-Hamiltonian *H* to obtain the Hamiltonian operator $\hat{H}$. The operators $\{\hat{x}, \hat{T}, \hat{p}_x, \hat{p}_T\}$ obey the the fundamental commutation relations

$$[\hat{x}, T] = [\hat{p}_x, \hat{p}_T] = [\hat{x}, \hat{p}_T] = [T, \hat{p}_x] = 0; \quad [\hat{x}, \hat{p}_x] = [\hat{T}, \hat{p}_T] = i\hbar. \tag{20}$$

Next, by imposing the constraint equation

$$\hat{H}\Psi(x, T) = 0\,, \tag{21}$$

we obtain, in our model, a Schrödinger-type equation,

$$-\frac{\partial^2\Psi(x,\tau)}{\partial x^2}+\left(m^2w_k^2-4m\Lambda x\right)\Psi(x,\tau)=2mi\frac{\partial\Psi(x,\tau)}{\partial\tau}, \quad (22)$$

in which we have redefined $T=-\tau$ and adopted $\hbar=1$.

We can now use the method of separation of variables, writing

$$\Psi_n(x,\tau)=\psi_n(x)\,e^{-iE_n\tau}, \quad (23)$$

and obtaining eigenfunctions $\psi_n(x)$ of the form

$$\psi_n(x)=C_1\,\mathrm{Ai}\left[\frac{\sqrt[3]{m}\left(mw_k^2-4\Lambda x-2E_n\right)}{2^{4/3}\Lambda^{2/3}}\right]+C_2\,\mathrm{Bi}\left[\frac{\sqrt[3]{m}\left(mw_k^2-4\Lambda x-2E_n\right)}{2^{4/3}\Lambda^{2/3}}\right]. \quad (24)$$

Here, $\mathrm{Ai}(x)$ and $\mathrm{Bi}(x)$ are the Airy functions. As $x\to\infty$, $\mathrm{Ai}(x)$ decays exponentially, whereas $\mathrm{Bi}(x)$ grows exponentially. Therefore, in order for (24) to be well-behaved as $x\to\infty$, we must let $C_2=0$, obtaining

$$\psi_n(x)\sim\mathrm{Ai}\left[\frac{\sqrt[3]{m}\left(mw_k^2-4\Lambda x-2E_n\right)}{2^{4/3}\Lambda^{2/3}}\right]. \quad (25)$$

These eigenstates must satisfy the boundary conditions

$$\psi_n(0)=\psi_n(\infty)=0. \quad (26)$$

The condition at $x\to\infty$ is already satisfied by *Ai*(*x*). The boundary condition at $x=0$ yields an equation for the energy eigenvalues E_n,

$$\mathrm{Ai}\left[\frac{\sqrt[3]{m}\left(mw_k^2-2E_n\right)}{2^{4/3}\Lambda^{2/3}}\right]=0. \quad (27)$$

Since the Airy's functions has known roots r_n, we straightforwardly write

$$E_n=\frac{m}{2}w_k^2-\sqrt[3]{\frac{2\Lambda^2}{m}}r_n. \quad (28)$$

By inserting (28) into (25), we get the eigenvectors

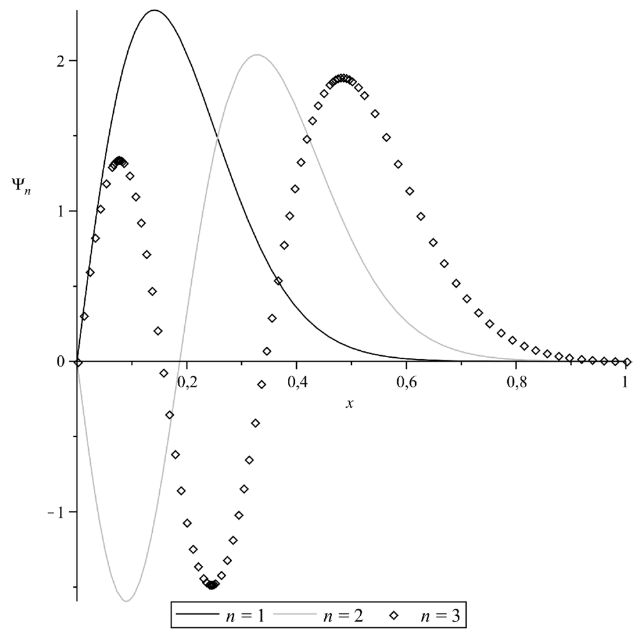

Fig. 1 Normalized eigenstates corresponding to the three lowest levels of energy. We let $\beta=0.27$, $\sigma=0.9999$, and $\Lambda=-15$. The eigenstates do not depend on the spatial curvature *k*, even though the eigenenergies do. (See main text.)

$$\psi_n(x)\sim\mathrm{Ai}\left[r_n-\sqrt[3]{4m|\Lambda|}\,x\right], \quad (29)$$

up to a normalization constant, determined by imposing $\int_0^\infty dx\,\psi_n^\star(x)\psi_n(x)=1$. Observe that the eigenfunctions (29) do not depend on the spatial curvature *k*, even though the energy levels (28) do. Even so, the dependence of the latter on *k* comes from w_k (Eq. (11)), and amounts to the constant term $mw_k^2/2$. Figure 1 shows the three lowest energy eigenstates, for all values of *k*.

Tables 1, 2, and 3 display the behavior of the eigenenergies corresponding to the first three energy levels as functions of the parameters *k* and Λ. The results indicate that the energy spectrum increases with larger values of *k* and larger values of $|\Lambda|$.

The quantum dynamics is expressed in terms of wave packets, built through the superposition of the eigenstates (25):

$$\Psi(x,\tau)=\sum_{n=1}^{N}C_n\,\mathrm{Ai}\left[r_n-\sqrt[3]{4m|\Lambda|}\,x\right]e^{-iE_n\tau}. \quad (30)$$

Table 1 The three lowest energy levels for $k=-1$, $\beta=0.27$ and $\sigma=0.9999$, for several different values of Λ

Level	$\Lambda=-15$	$\Lambda=-10$	$\Lambda=-5$	$\Lambda=-1$
E_1	1.501711858	−0.275264523	−2.393864681	−4.767113911
E_2	7.116449950	4.009582590	0.305419853	−3.843971585
E_3	11.71328324	7.517622940	2.515346793	−3.088187203

Table 2 The three lowest energy levels for $k = 0$, $\beta = 0.27$ and $\sigma = 0.9999$, for several different values of Λ

Level	$\Lambda = -15$	$\Lambda = -10$	$\Lambda = -5$	$\Lambda = -1$
E_1	7.502311918	5.725335537	3.606735379	1.1534
E_2	13.11705001	10.01018265	6.306019913	3.1377
E_3	17.71388330	13.51822300	8.515946853	5.1642

Table 3 The three lowest energy levels for $k = 1$, $\beta = 0.27$ and $\sigma = 0.9999$, for several different values of Λ

Level	$\Lambda = -15$	$\Lambda = -10$	$\Lambda = -5$	$\Lambda = -1$
E_1	13.50291198	11.72593560	9.607335439	7.234086209
E_2	19.11765007	16.01078271	12.30661997	8.157228535
E_3	23.71448336	19.51882306	14.51654691	8.913012917

The coefficients C_n are arbitrary up to the normalization of the package, imposed by $\int_0^\infty dx\ \Psi(x,\tau)^*\Psi(x,\tau) = 1$, for all $\tau \geq 0$.

Like the eigenstates, all wave packets should satisfy the boundary conditions given in (26). And yet, they are normalizable, showing a constant and well defined norm in all space, even when $x \to 0$.

The probability density can be written as

$$\rho(x,\tau) = |\Psi(x,\tau)|^2 \\ = \sum_{n=1}^{N}\sum_{j=1}^{N} C_n^\star C_j \ \mathrm{Ai}\left[r_n - \sqrt[3]{4m|\Lambda|}\ x\right] \\ \mathrm{Ai}\left[r_j - \sqrt[3]{4m|\Lambda|}\ x\right]\cos\left[(E_n - E_j)\tau\right]. \tag{31}$$

The energy levels E_n (28) depend on the spatial curvature k through w_k, but the energy eigenstates $\psi_n(x)$ (29) do not. The wave packets (30) depend on k but only through a global phase $e^{-imw_k^2\tau/2}$; consequently, the probability density (31) *does not* depend on k. (Equivalently: it depends on the physically observable energy differences $E_n - E_m$, which are independent of k.) In addition, the expectation values of position and momentum will also be independent of k.

Figure 2 shows the probability density related to wave packets (30) built out of the equiprobable superposition of the three lowest energy levels, corresponding to any spatial curvature $k \in \{-1, 0, 1\}$, with normalized coefficients $C_n = 0.9999333362599749$, for all n. In panel (a), there is a pronounced probability peak near $x = 0$, accompanied by gentle oscillations that decay rapidly as $x \to \infty$; this behavior reflects the imposed boundary conditions $\Psi(0,\tau) = \Psi(\infty,\tau) = 0$, which enforce the vanishing of the wave function at the endpoints. The packet's profile suggests a coherent superposition of the lowest-lying quantum states, with constructive interference near the origin. In panel (b), the packet broadens, and the main peak shifts slightly toward larger values of x; more well-defined secondary oscillations emerge, indicating increased contributions from higher-energy states to the superposition. In panel (c), the packet becomes more dispersed, with multiple probability maxima distributed along x. The amplitude of the main peak gets smaller, whereas the secondary oscillations gain strength, evidencing quantum dispersion and interference among the superposed states. Finally, panel (d) shows that the packet reaches its maximal dispersion within the analyzed interval, with the probability density becoming nearly uniform over a broad region of x. The secondary oscillations get more numerous and smaller in amplitude, indicating that the packet approaches a stationary configuration. The absence of a dominant peak, along with the presence of multiple low-amplitude oscillations, suggests that the packet no longer drifts appreciably, but instead oscillates around an average configuration.

4 Results

4.1 The Many-worlds Interpretation

The wave function of the Universe $\Psi(x,\tau)$ is a superposition of stationary eigenstates $\Psi_n(x)$, each one associated with an eigenvalue E_n. In the many-worlds interpretation of quantum mechanics, originally proposed by Everett [48, 49], each eigenstate $\Psi_n(x)$ is regarded as representative of a distinct "branch" of the Universe, corresponding to different dynamical configurations of the scale factor $x(\tau)$ and of the cosmic-string fluid. This viewpoint is particularly relevant in the context of the Wheeler–DeWitt equation (22), which is independent of an external time parameter, suggesting that the classical notion of temporal evolution emerges only locally within each branch.

The behavior of scale factor the Universe is described by the evolution of its expectation value,

$$\langle x(\tau)\rangle = \frac{\int_0^\infty \Psi^\star(x,\tau)\ x\ \Psi(x,\tau)dx}{\int_0^\infty \Psi^\star(x,\tau)\Psi(x,\tau)dx}, \tag{32}$$

following the same procedure as in the Copenhagen interpretation. Quantum fluctuations may occur in the scale factor in the early Universe. The uncertainty $\delta(\tau)$ is defined as

$$\delta(\tau) = \sqrt{\langle x(\tau)^2\rangle - \langle x(\tau)\rangle^2}, \tag{33}$$

so that the range of variation of the scale factor $\langle x(\tau)\rangle$ is given by $[\Delta_-(\tau), \Delta_+(\tau)]$, in which

$$\Delta_\pm(\tau) = \langle x(\tau)\rangle \pm \delta(\tau). \tag{34}$$

Figure 3 compares the scale factor expectation value $\langle x(\tau)\rangle$ (black line) and $\Delta_\pm(\tau)$ (grey lines) for all values of

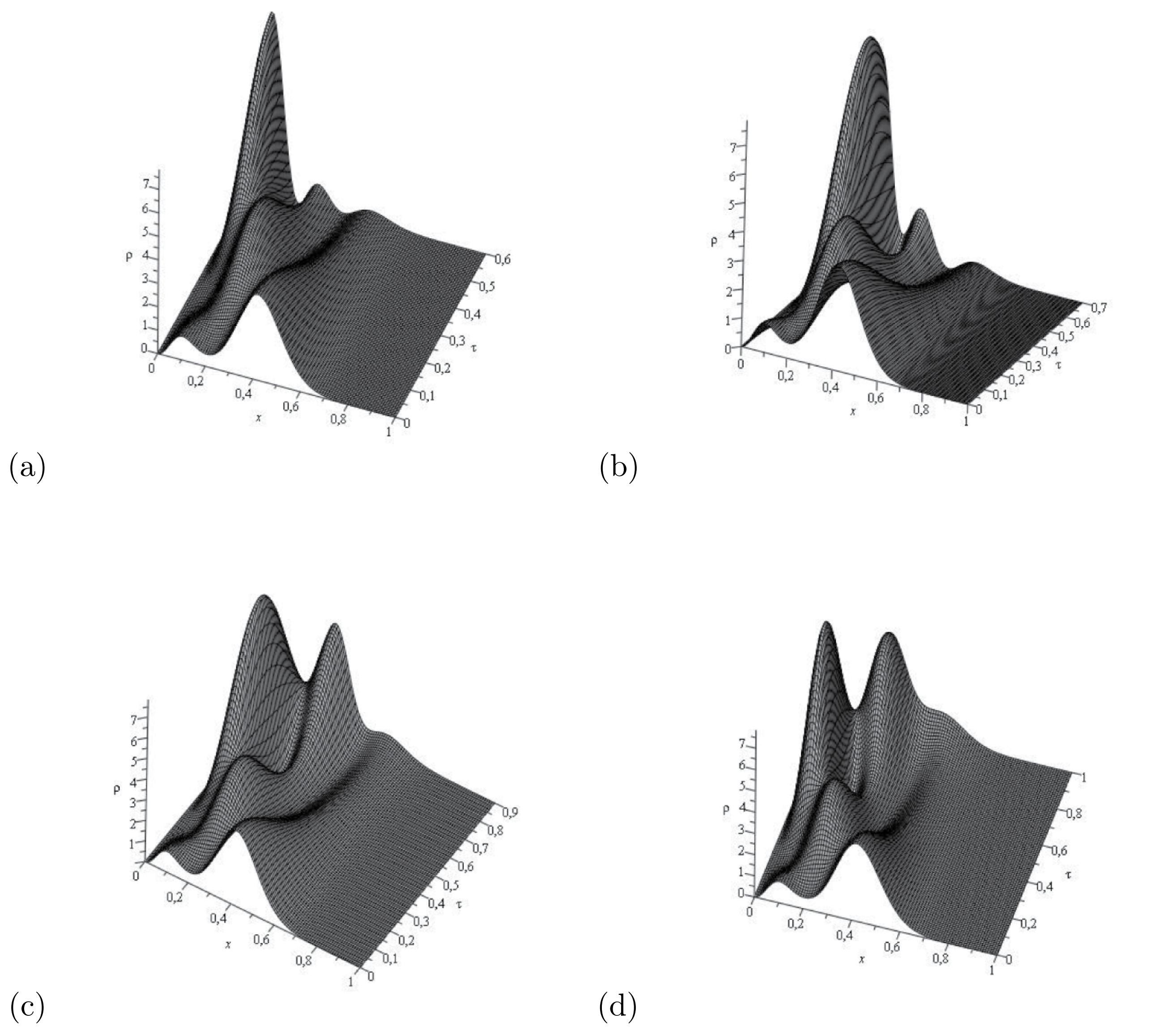

Fig. 2 Time evolution of the probability density associated to wave packets, for $\tau \in [0, \delta\tau]$, for values of $\delta\tau$: (**a**) $\delta\tau = 0.6$; (**b**) $\delta\tau = 0.7$; (**c**) $\delta\tau = 0.9$; and (**d**) $\delta\tau = 1$. Here we let $\beta = 0.27$, $\sigma = 0.9999$, and $\Lambda = -15$. The same evolution occurs for all values of the spatial curvature, $k \in \{-1, 0, 1\}$

k. We have $\min_\tau \Delta_-(\tau) = 0.008657875868247095 \neq 0$; therefore, we can assert that there is no singularity at the quantum level, for the present model.

4.2 The de Broglie-Bohm Interpretation

The de Broglie-Bohm interpretation [50, 51] of quantum mechanics, originally proposed by Louis de Broglie and further developed by David Bohm, asserts that particles possess well-defined positions at all times, guided by a "pilot wave" represented by the wave function $\Psi(x, \tau)$. In this interpretation, reality is deterministic: particles follow precise, albeit hidden, trajectories, with quantum randomness emerging solely from ignorance of initial conditions. The wave function does not collapse but rather acts as a real physical field that influences particles. Non-locality is intrinsic, reflecting instantaneous action between entangled particles (as in the EPR experiment), consistent with Bell's theorem. This view preserves ontological realism (i.e., that particles exist independently of measurement).

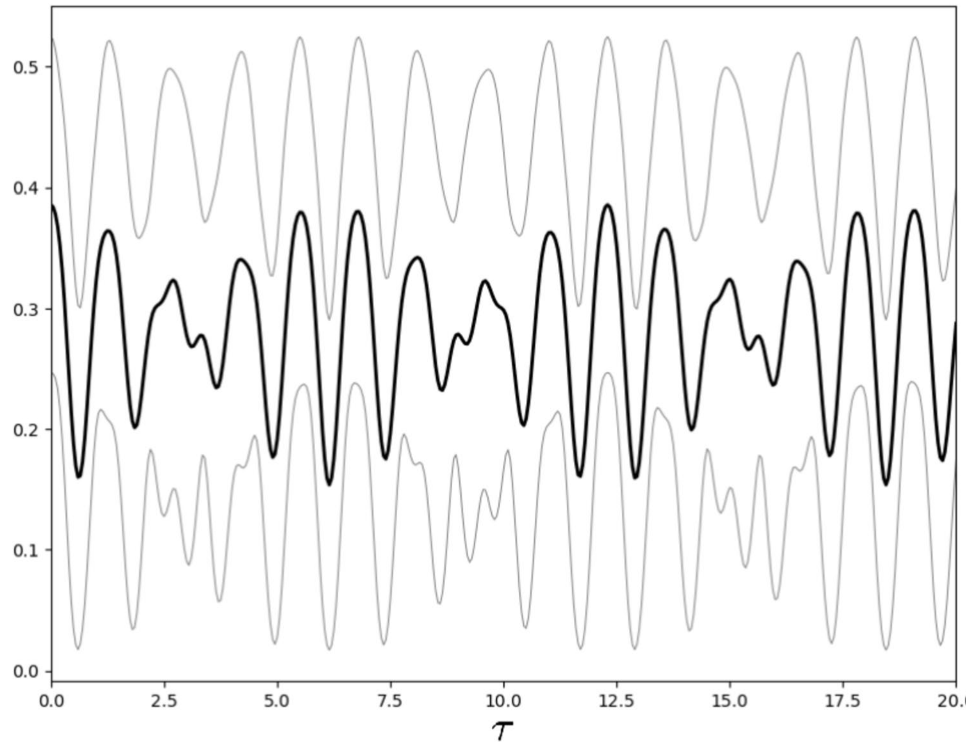

Fig. 3 Behavior of $\langle x(\tau)\rangle$ (black central line) and fluctuations $(\Delta_{\pm}(\tau))$ (upper and lower gray lines, respectively) as functions of time τ, for all values of the spatial curvature k. We let $\beta = 0.27$, $\sigma = 0.9999$ and $\Lambda = -15$

According to the postulates of the de Broglie–Bohm interpretation, we assume the following.

1. The wave function $\Psi(x,\tau)$ obeys the unitary dynamics generated by the Wheeler–DeWitt equation.
2. Writing $\Psi(x,\tau)$ in polar form, $\Psi(x,\tau) = \mathcal{R}(x,\tau)\, e^{i\mathcal{S}(x,\tau)}$, the phase $S(x,\tau)$ satisfies a modified Hamilton–Jacobi equation in which an extra potential term encodes the quantum corrections,

$$Q = -\frac{1}{\mathcal{R}(x,\tau)}\frac{\partial^2\mathcal{R}}{\partial x^2}\,. \tag{35}$$

3. The scale factor $x(\tau)$ is an ontological variable, the momentum of which is defined by the guiding equation

$$p_x = \frac{\partial\mathcal{S}}{\partial x}\,. \tag{36}$$

In our model, by rewriting the wave function of the Universe (30) as

$$\begin{aligned}\Psi(x,\tau) = &\sum_{n=1}^{N} C_n \text{ Ai}\left[r_n - \sqrt[3]{4m|\Lambda|}\; x\right]\cos(E_n\tau) \\ &-i\sum_{n=1}^{N} C_n \text{ Ai}\left[r_n - \sqrt[3]{4m|\Lambda|}\; x\right]\sin(E_n\tau)\,,\end{aligned} \tag{37}$$

and using (31) and (37) it is possible to identify $\mathcal{R}(x,\tau)$ and $\mathcal{S}(x,\tau)$ as

$$\begin{aligned}\mathcal{R}(x,\tau) = &\sum_{n=1}^{N}\sum_{j=1}^{N} C_n^{\star}C_j \text{ Ai}\left[r_n - \sqrt[3]{4m|\Lambda|}\; x\right] \\ &\text{Ai}\left[r_j - \sqrt[3]{4m|\Lambda|}\; x\right]\cos\left[(E_n - E_j)\tau\right]\end{aligned} \tag{38}$$

and

$$\mathcal{S}(x,\tau) = \arctan\left[\frac{\sum_{n=1}^{N} C_n^{\star}\text{Ai}\left[r_n - \sqrt[3]{4m|\Lambda|}\; x\right]\sin(E_n\tau)}{\sum_{j=1}^{N} C_j\text{Ai}\left[r_j - \sqrt[3]{4m|\Lambda|}\; x\right]\cos(E_j\tau)}\right], \tag{39}$$

which amounts to

$$\frac{\partial S}{\partial x} = \frac{\sum_{n=1}^{N}\sum_{m=1}^{N} \lambda\, C_n C_m \text{ Ai}'(\theta_n)\text{Ai}(\theta_m)\sin\left[(E_n - E_m)\tau\right]}{\sum_{n=1}^{N}\sum_{m=1}^{N} C_n C_m \text{ Ai}(\theta_n)\text{Ai}(\theta_m)\cos\left[(E_n - E_m)\tau\right]} \tag{40}$$

with

$$\theta_k = r_k - \sqrt[3]{4m|\Lambda|}x \tag{41}$$

and

$$\lambda = \frac{-4\Lambda\sqrt[3]{m}}{2^{4/3}\Lambda^{2/3}} = -\sqrt[3]{4m|\Lambda|}. \tag{42}$$

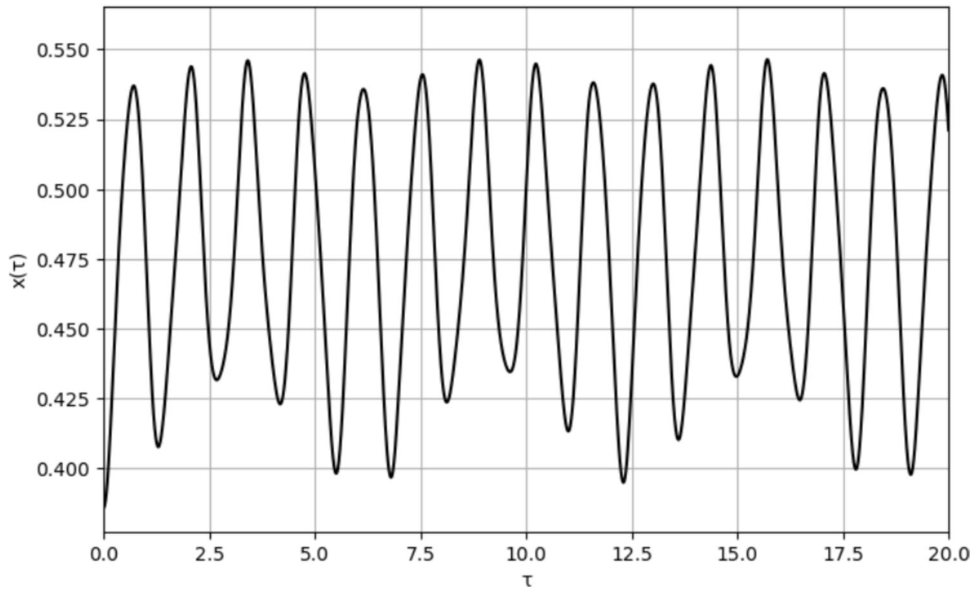

Fig. 4 Bohmian trajectory $x_{Bohm}(\tau)$ for $\tau \in [0, 20]$, for all values of the spatial curvature *k*, obtained for $\Lambda = -15, \sigma = 0.9999$ and $\beta = 0.27$

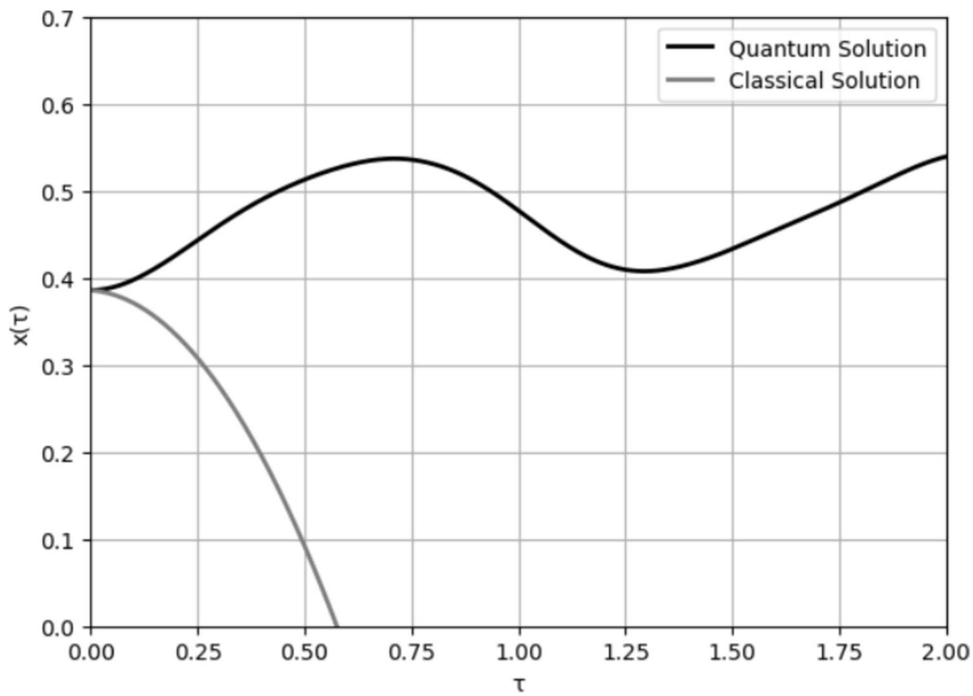

Fig. 5 Comparison between the classical solution (gray lower line) and the Bohmian trajectory (black upper line) for the scale factor, for $\tau \in [0, 2]$. The classical solution quickly collapses, whereas the quantum solution oscillates within a finite range of non-vanishing values. We let $\beta = 0.27$, $\sigma = 0.9999$, $\Lambda = -15$. Both solutions are insensitive to the spatial curvature *k*

Observe that neither $\mathcal{R}(x, \tau)$ (38) nor $\mathcal{S}(x, \tau)$ (40) depend on the spatial curvature *k*, since those expressions depend on the physically observable energy differences $(E_n - E_m)$, which are insensitive to *k*.

The Bohmian trajectories $x(\tau)$, which describe the behavior of the scale factor, are solutions of the ODE

$$\frac{dx(\tau)}{d\tau} = -\frac{1}{m}\frac{\partial \mathcal{S}(x, \tau)}{\partial x}, \tag{43}$$

Using the expectation value (32) at $\tau = 0$ as the initial condition for (43), i.e., letting $x_{\text{Bohm}}(0) = \langle x(0) \rangle_{MW} = 0.3858647063 63$, one obtains the solution depicted in Fig. 4. It portrays Universes with a scale factor that oscillates between finite non-vanishing values. Just like in the many-worlds interpretation, this model is free from singularities at the quantum level.

Comparing the Bohmian trajectory with the classical solution (18) under the same initial condition, one concludes that they quickly drift apart, as shown in Fig. 5 for $\tau \in [0, 2]$.

The quantum potential $Q(x_{Bohm}(\tau))$ evaluated along the Bohmian trajectories $x_{\text{Bohm}}(\tau)$ can be calculated from (35) and (38). Also insensitive to the spatial curvature *k*, the

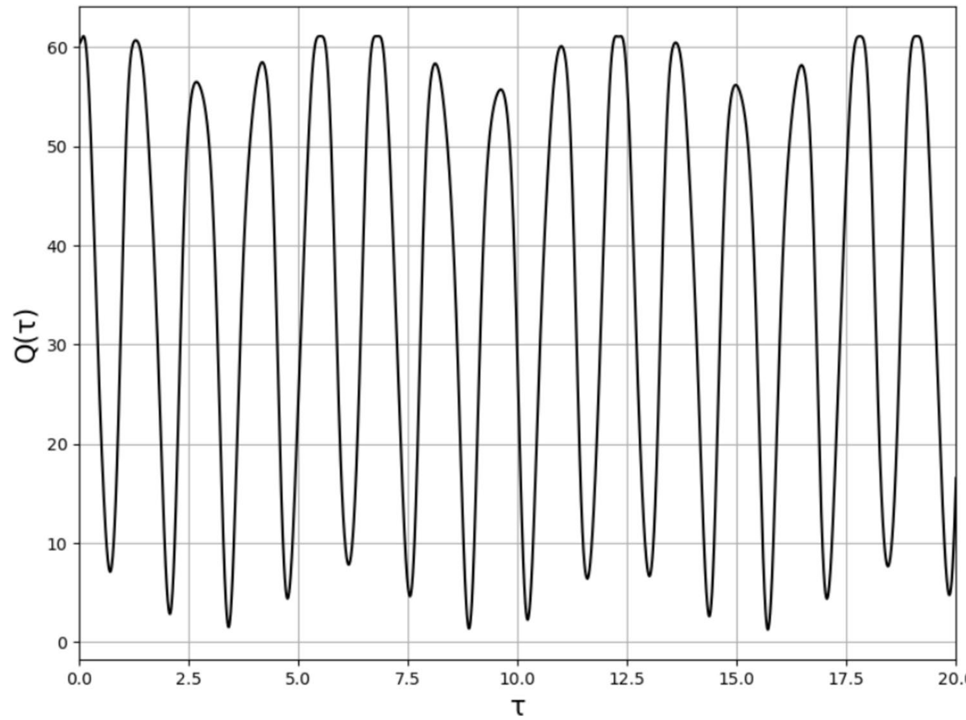

Fig. 6 The quantum potential $Q(x_{Bohm}(\tau))$ computed over the Bohmian trajectory $x_{Bohm}(\tau)$ for $\tau \in [0, 20]$. It is insensitive to the value of the spatial curvature k

quantum potential acts repulsively, thereby preventing singularities, as shown in Fig. 6.

5 Conclusions

We developed a FLRW model within Einstein–Æther gravity with a negative cosmological constant and a cosmic string fluid as its matter content. Starting from the canonically reduced action, we derived the super-Hamiltonian and obtained singular classical solutions for the scale factor of the Universe. At the quantum level, the Wheeler-DeWitt equation takes the form of a Schrödinger-type equation. Its stationary solutions are normalizable superpositions of Airy functions that satisfy the imposed boundary conditions. Using these wave packets, we investigated the quantum dynamics of the scale factor in both the many-worlds (using its expectation value) and the de Broglie-Bohm interpretations (using its Bohmian trajectories). The wave–packet profiles are independent of the spatial curvature of the model. Both interpretations consistently predict singularity avoidance. In particular, the quantum potential evaluated along the Bohm trajectories acts repulsively and provides the mechanism for such avoidance.

The quantum solutions obtained behave independently of the spatial curvature. This feature seems to stem from the specific role the cosmic string fluid plays in our model's Hamiltonian and Wheeler–DeWitt equation. This result indicates that the presence of such fluid may smooth out or even neutralize the direct influence of spatial curvature on the quantum dynamics of the primordial Universe.

In a future work, we will test the robustness of this effect by replacing the cosmic string fluid with other barotropic fluids. This will allow us to understand how different material contents modify the solution structure and singularity avoidance mechanisms within Einstein–Æther theory.

Author Contributions All authors contributed equally to the conception and elaboration of this manuscript.

Funding The Article Processing Charge (APC) for the publication of this research was funded by the Coordenação de Aperfeiçoamento de Pessoal de Nível Superior - Brasil (CAPES) (ROR identifier: 00x0ma614). G. A. Monerat thanks FAPERJ for partial financial support. G.A. Monerat, E. V. Corrêa Silva and J. C. G. Tedesco thank Universidade do Estado do Rio de Janeiro, UERJ, for the Prociência grant. A. Oliveira Castro Júnior, V. J. Monteiro and F. R. Manhães thank CAPES for financial support. This study was financed in part by the Coordenação de Aperfeiçoamento de Pessoal de Nível Superior "Brasil (CAPES)" Finance Code 001. F. G. Alvarenga thanks the Sci-Com Lab of the Department of Physics at UFES, which was funded by FAPES (Brazil, TO 1081/2022). G. Oliveira-Neto thanks FAPEMIG (APQ-06640-24) for partial financial support. The Article Processing Charge (APC) for the publication of this research was covered by the Coordenação de Aperfeiçoamento de Pessoal de Nível Superior – CAPES (ROR ID: 00x0ma614). For open access purposes, the authors have applied a Creative Commons Attribution (CC BY) license to any accepted manuscript version arising from this submission.

Data Availability No datasets were generated or analysed during the current study.

Declarations

Competing Interests The authors declare no competing interests.

Ethical Approval Not applicable in our research shown here.

References

1. J.A. Halliwell, Quantum cosmology and baby universes. ed. World Scientific, (1991)
2. M. Bojowald, Quantum cosmology: a review. Rep. Prog. Phys. **78**, 023901 (2015). arXiv:1501.04899 [gr-qc]
3. P. V. Moniz, Quantum Cosmology - The Supersymmetric Perspective - vol. 1: Fundamentals (Lecture Notes in Physics). Springer, (2010)
4. R. Arnowitt, S. Deser e C.W. Misner, Gravitation: An Introduction to Current Research, Wiley, New York (1962)
5. B.S. DeWitt, Phys. Rev. **160**, 1113 (1967)
6. F.G. Alvarenga, J.C. Fabris, N.A. Lemos, G.A. Monerat, Quantum cosmological perfect fluid models. Gen. Rel. Grav. **34**, 651–663 (2002). arXiv:gr-qc/0106051v2
7. D. Mattingly, Living Reviews in Relativity 8 (1), (2005)
8. T. Jacobson, D. Mattubgly, Phys. Re. D, **64** (2), (2001)
9. T. Jacobson, Einstein-Aether gravity: a status report. arXiv **0801**, 1547 (2008)
10. S.M. Carroll, E. Lim, Phys. Rev. D **70**, 123525 (2004)
11. E. Lim, Phys. Rev. D **71**, 063504 (2005)
12. S.M. Carroll, J. Shu. Phys. Rev. D **73**, 103515 (2006)
13. R. Chan, M. F. A. da Silva, V.H. Satheeshkumr, Existence of new singularities in Einstein-Aether theory. JCAP 05 (2020)025. arXiv:1912.12845 [gr-qc]
14. M. Khodadi, E.N. Saridakis, Einstein-Æther gravity in the light of event horizon telescope observations of M87*. Physics of the Dark Universe **32**, 100835 (2021). https://doi.org/10.1016/j.dark.2021.100835
15. A. H. Bokhari, J. Rayimbaev, B. Ahmedov, Radio loudness and spindown of pulsars in Einstein-aether gravity. Physics of the Dark Universe **34** 100901 (2021). DOI: https://doi.org/10.1016/j.dark.2021.100901
16. M. Bairagi, Parametrizations of dark energy model in the background of non-canonical scalar field in Einstein-Aether Gravity. Physics of the Dark Universe **39**, 101158 (2023). https://doi.org/10.1016/j.dark.2022.101158
17. A. Adam, P. Figueras, T. Jacobson, T. Wiseman, Rotating black holes in Einstein-aether theory. Class. Quantum Gravity **39**, 125001 (2022). https://doi.org/10.1088/1361-6382/ac5053
18. G. Oliveira-Neto, No boundary wave function of the anti-de Sitter space-time and the quantization of Lambda. Physical Review D **58**, 107501 (1998). https://doi.org/10.1103/PhysRevD.58.107501
19. P. Pedram, M. Mirzaei, S. Jalalzadeh, S.S. Gousheh, Perfect fluid quantum Universe in the presence of negative cosmological constant. Gen. Rel. Grav. **40**, 1663–1681 (2008). arXiv:0711.3833v1 [gr-qc]
20. G. A. Monerat, L. G. Ferreira Filho, G. Oliveira-Neto, E.V. Corrêa Silva, C. Nevesa. The Planck era with a negative cosmological constant and cosmic strings. Physics Letters A 374 (2010) 4741–4745
21. G. Oliveira-Neto, G.A. Monerat, E.V. Corrêa Silva, C. Neves, L.G. Ferreira Filho, Quantization of Friedmann-Robertson-Walker Spacetimes in the Presence of a Cosmological Constant and Stiff Matter. Int. J. Theor. Phys. **52**9, 2991–3006 (2013) . https://doi.org/10.1007/s10773-013-1590-7.
22. G. A. Monerat, F. G. Alvarenga, G. Oliveira-Neto et al. Wormholes-like solutions in quantum cosmology with radiation, negative cosmological constant and Pöschl–Teller potential. Eur. Phys. J. Plus **140**, 320 (2025). https://doi.org/10.1140/epjp/s13360-025-06257-5
23. Ö. Akarsu, A. De Felice, E. Di Valentino, S. Kumar, R.C. Nunes, E. Özülker, J.A. Vazquez, A. Yadav, Cosmological constraints on Λs CDM scenario in a type II minimally modified gravity. PHYSICAL REVIEW D 110, 103527 (2024). https://doi.org/10.1103/PhysRevD.110.103527
24. N. Menci, A. A. Sen, M. Castellano, The Excess of JWST Bright Galaxies: A Possible Origin in the Ground State of Dynamical Dark Energy in the Light of DESI 2024 Data. The Astrophysical Journal, 976:227 (8pp), 2024 December. https://doi.org/10.3847/1538-4357/ad8d5b
25. C.B. Dash, T. Guha Sarkar, A.A. Sen, Post-reionization HI 21-cm signal: a probe of negative cosmological constant. MNRAS **527**, 11694–11706 (2024). https://doi.org/10.1093/mnras/stad3946
26. N. Menci, S. A. Adil, U. Mukhopadhyay, A. A. Sen, S. Vagnozzi, Negative cosmological constant in the dark energy sector: tests from JWST photometric and spectroscopic observations of high-redshift galaxies
27. S. A. Adil, U. Mukhopadhyay, A. A. Sen, S. Vagnozzi, Dark energy in light of the early JWST observations: case for a negative cosmological constant?
28. B.F. Schutz, Perfect fluids in General Relativity: Velocity potentials and a variational principle. Phys. Rev. D **2**, 2762–2773 (1970)
29. B.F. Schutz, Hamiltonian theory of a relativistic perfect fluid. Phys. Rev. D **4**, 3559–3566 (1971)
30. F.G. Alvarenga, R.G. Furtado, R. Fracalossi, S.V.B. Gonçalves, Braz. J. Phys. **47**, 96 (2016)
31. T.W.B. Kibble, Topology of cosmic domains and strings. J. Phys. A: Math. Gen. **9**(8), 1387–1398 (1976)
32. A. S. Lo, E. L. Wright, Signatures of Cosmic Strings in the Cosmic Microwave Background. arXiv:astro-ph/0503120v1
33. M. Wyman, L. Pogosian, I. Wasserman, Bounds on Cosmic Strings from WMAP and SDSS. Phys.Rev.D72:023513,2005. http://arxiv.org/abs/astro-ph/0503364v2
34. C. Dvorkin, M. Wyman, W. Hu, Cosmic String constraints from WMAP and the South Pole Telescope. Phys.Rev.D.84:123519, (2011). arXiv:1109.4947v2 [astro-ph.CO]
35. P. Collaboration, Planck, results (XXV, Searches for cosmic strings and other topological defects, 2013). arXiv:1303.5085 [astro-ph.CO]
36. G. A. Monerat, C. G. M. Santos, F. G. Alvarenga, S. V. B. Gonçalves, R. Fracalossi, E. V. Corrêa Silva, G. Oliveira-Neto. Quantum Cosmology with many fluids and the choice of cosmological time.Brazilian Journal of Physics, **50**, 89–104 (2020). arXiv:1908.05337v2 [gr-qc]

37. L. Visinelli, S. Vagnozzi, U. Danielsson, Symmetry **11**, 1035 (2019). arXiv:1907.07953 [astro-ph.CO]
38. S.A. Adil, U. Mukhopadhyay, A.A. Sen, S. Vagnozzi, Dark energy in light of the early JWST observations: case for a negative cosmological constant? JCAP **2310**, 072 (2023). arXiv:2307.12763v3 [astro-ph.CO]
39. C.B.V. Dash, T.G. Sarkar, A.A. Sen, Mon. Not. R. Astron. Soc. **527**(4), 11694–11706 (2024). arXiv:2309.01623v2 [astro-ph.CO]
40. N. Menci, S.A. Adil, U. Mukhopadhyay, A.A. Sen, S. Vagnozzi, Negative cosmological constant in the dark energy sector: tests from JWST photometric and spectroscopic observations of high-redshift galaxies. JCAP **2407**, 072 (2024). arXiv:2401.12659v2 [astro-ph.CO]
41. H. Wang, Z.-Y. Peng, Y.-S. Piao, Can recent DESI BAO measurements accommodate a negative cosmological constant? arXiv:2406.03395v2 [astroph. CO]
42. V.G. Lapchinskii, V.A. Rubakov, Theor. Math. Phys. **33**, 1076 (1977)
43. F.G. Alvarenga, L.A.M. Diniz, S.V.B. Gonçalves, G.A. Monerat, E.V.C. Silva, Observational constraints on the quantum Einstein-Aether model. European Physical Journal Plus **138**, 1–13 (2023)
44. G.A. Monerat, O. Goldoni, F.G. Alvarenga, G. Oliveira-Neto, E.V.C. Silva, Quantum cosmological perfect fluid models in Einstein aether theory. European Physical Journal Plus **137**, 1–9 (2022)
45. G. A. Monerat, F. G. Alvarenga, G. Oliveira-Neto, E. V. Corrêa Silva, J. C. G. Tedesco and F. R. Manhães, Quantum cosmological models in the Einstein-aether theory with radiation fluid. European Physical Journal Plus, v. 139, p. 1-11 (2024)
46. B.S. DeWitt, Phys. Rev. **160**, 1113 (1967)
47. P.A.M. Dirac, *Lectures on Quantum Mechanics* (Yeshiva University Press, New York, 1964)
48. H. Everett, III. The Many-Worlds Interpretation of Quantum Mechanics, ed. by B. S. DeWitt and N. Graham (Princeton University Press, Princeton, 1973)
49. F., J. Tipler, Phys. Rep. **137**, 231 (1986)
50. D. Bohm, J. B. Hiley, The Undivided Universe: An Ontological Interpretation of Quantum Theory (Taylor & Francis Ltd,) (1995)
51. P.R. Holland, *The Quantum Theory of the Motion: AnAccount of the de Broglie-Bohm Interpretation of Quantum Mechanics* (Cambridge University Press, Cambridge, 1993)